

# Miniaturized thermoelectric generators based on poly-Si and poly-SiGe surface micromachining

M. Strasser<sup>a,b,\*</sup>, R. Aigner<sup>a</sup>, M. Franosch<sup>a</sup>, G. Wachutka<sup>b</sup>

<sup>a</sup>*Infineon Technologies AG, Wireless Products, WS TI Microsystems, 81730 München, Germany*

<sup>b</sup>*Institute for Physics of Electrotechnology, Munich University of Technology, 80290 München, Germany*

Received 3 July 2001; received in revised form 25 October 2001; accepted 7 November 2001

## Abstract

We report on miniaturized thermoelectric generators (TEGs) which are being developed to convert waste heat into a few microwatts of electrical power, sufficient to supply microelectronic circuitry. A BiCMOS realization using standard materials is favored to make these generators amenable to low cost applications. In order to optimize our device, the design and the material properties have been studied. The use of micromachining techniques allowed us to improve the thermal efficiency of the generator significantly. Low thermal conductivity of the thermoelectric materials proved to be the most important factor to increase the output power. The materials we have investigated are poly-Si and poly-SiGe. Experimental results obtained from fabricated devices show good agreement with the predictions of thermal simulations. © 2002 Elsevier Science B.V. All rights reserved.

**Keywords:** Thermoelectric generator; Figure of merit; Thermal conductivity; Surface micromachining; Poly-Si; Poly-SiGe

## 1. Introduction

For the operation of small electronic devices and systems, a power supply of some few microwatts is sufficient in various cases. If there is a thermal gradient between the location of the device and the ambient, the batteries of such systems could be replaced by attached thermoelectric generators (TEGs). For example, we usually find a temperature difference of some degrees between the surface of the human body and its environment. Exploiting this temperature gradient, wrist watches can be powered thermoelectrically [1]. Some other environments such as heating appliances (e.g. radiators) or engines in the automotive field provide even higher thermal differences.

Our goal is to develop a micromachined TEG that matches the needs of low cost, small size and low power systems. Therefore, we explore BiCMOS materials such as poly-Si and poly-SiGe for our thermoelectric applications. Since these materials are compatible with the fabrication process, our generator can be easily integrated on chip-level.

## 2. Basic considerations

Although several theoretical calculations already exist to describe the performance of Seebeck effect based power generators and Peltier effect based cooling devices [2,3] there is still some need of understanding the behavior of micro-scale waste heat TEGs [4] as shown schematically in Fig. 1. As conventional TEGs, too, such a device consists of couples of legs made of n- and p-type thermoelectric materials. These legs are electrically connected in series via metal bridges and are arranged in meanders to make best use of the given area. The actual generator layer is sandwiched between the silicon substrate below and a convection-cooled heat sink mounted on top. A thermal gradient between the bottom of the device and the ambient on top of it creates a vertical heat flow, which can be partly converted into electrical energy by the thermoelectric effects. The main difference to conventional, large-size TEGs lies in the small internal thermal resistance of the generator itself compared to the large thermal resistors enclosing it. Because of the dominance of the thermal resistors enclosing the device, the system is operated under constant heat flow conditions rather than at a constant temperature difference. For the theoretical analysis of this behavior, the thermal network of the device (see Fig. 2) has to be solved.

For a given relative Seebeck coefficient  $\alpha$  of the two thermoelectric materials employed, the generated open-circuit

\* Corresponding author. Tel.: +49-89-234-57409;

fax: +49-89-234-41848.

E-mail address: marc.strasser@infineon.com (M. Strasser).

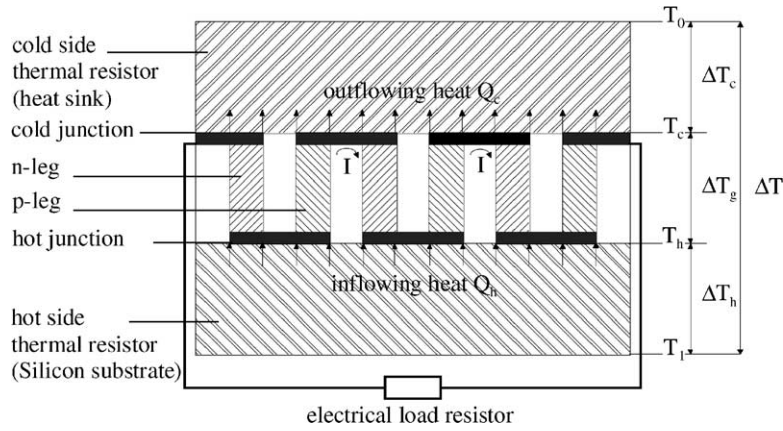


Fig. 1. Schematic cross-section of a generator with n- and p-doped thermoelectric legs.

voltage  $U_0$  can be expressed by the number of couples of thermoelectric legs  $m$  and the temperature difference  $\Delta T_g$  between the hot and the cold junctions:

$$U_0 = m\alpha \Delta T_g \quad (1)$$

As the system shall be operated at maximum electrical power output  $P_{out}$ , we have to match the electrical impedances in such a way that the Ohmic resistance of the generator is equal to the electrical resistance of the load:

$$P_{out} = U_{out}I = \frac{U_0^2}{4R_g} = \frac{m^2\alpha^2}{4R_g} (\Delta T_g)^2 \quad (2)$$

where  $U_{out}$  is the output voltage under load,  $I$  the electrical current and  $R_g$  is the electrical resistance of the generator.

In order to determine  $\Delta T_g$ , the thermoelectric network of the generator device will be solved in analogy to an electrical circuit in which the additional thermal resistors on the hot and cold side of the actual generator have to be taken into account. The aim is to define a figure of merit for the generator just depending on the material properties. First, a complete thermoelectric network will be derived including the Peltier effect and Joule heating (see Fig. 2). Next, instead of giving the solution to the general problem explicitly, a simplified model will be developed.

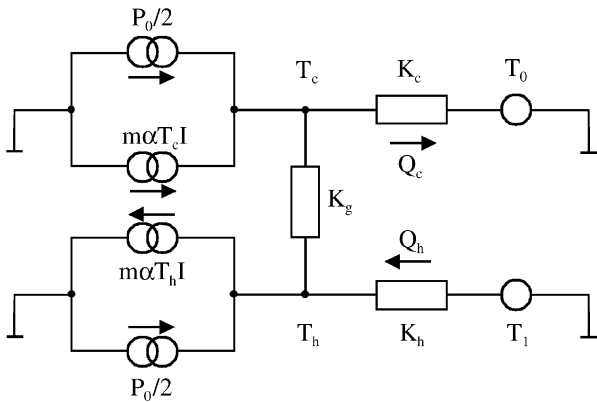


Fig. 2. Thermal network of a  $\mu$ -TEG including the Peltier effect and Joule heating.

### 2.1. Complete thermal network

In contrast to previous approaches, the total temperature drop  $\Delta T$  rather than  $\Delta T_g$  will be assumed to be given. If the generator is sandwiched between layers with thermal resistances  $K_c$  and  $K_h$  at the cold and hot side, respectively the individual temperature drops have to be added and can be expressed in terms of the corresponding heat currents  $Q_c$  and  $Q_h$ :

$$\Delta T = \Delta T_g + \Delta T_c + \Delta T_h = \Delta T_g + K_c Q_c + K_h Q_h \quad (3)$$

With the assumptions that the Seebeck coefficient  $\alpha$ , the electrical resistivity  $\rho$  and the thermal conductivity  $\lambda$  are independent of temperature, the heat currents in a thermoelectric device can also be treated independently [2]. The energy balances for the cold and hot side must include the heat contributions by the Peltier effect and the Joule heating in the generator. As the Joule heat generated in the legs follows its own temperature gradient it may be divided in two parts with one half being conducted to the cold end and one half conducted to the hot end of the leg. The sum of the heat current  $Q_h$  entering the hot junction at temperature  $T_h$  plus the Joule heat  $P_{out}/2$  is equal to the sum of the heat passing the generator  $\Delta T_g/K_g$  and the heat transformed into electrical power by the Peltier effect at the hot junction:

$$Q_h = \frac{\Delta T_g}{K_g} + m\alpha T_h I - \frac{P_{out}}{2} \quad (4)$$

where  $K_g$  is the thermal resistance of the generator itself.

The heat current  $Q_c$  leaving the cold junction at temperature  $T_c$  is composed of the heat passing the generator  $\Delta T_g/K_g$ , the heat released by the Peltier effect at the cold junction and the Joule heat:

$$Q_c = \frac{\Delta T_g}{K_g} + m\alpha T_c I + \frac{P_{out}}{2} \quad (5)$$

Substituting  $U_0/2R_g$  for the electrical current  $I$  in the case of matched impedances,  $T_l - K_h Q_h$  for  $T_h$  and  $T_0 + K_c Q_c$  for

$T_c$  and solving for the heat current yields:

$$Q_h = \frac{2R_g}{2R_g + m^2\alpha^2 K_h \Delta T_g} \left( \frac{\Delta T_g}{K_g} + \frac{m^2\alpha^2 T_1 \Delta T_g}{2R_g} - \frac{P_{out}}{2} \right) \quad (6)$$

$$Q_c = \frac{2R_g}{2R_g - m^2\alpha^2 K_c \Delta T_g} \left( \frac{\Delta T_g}{K_g} + \frac{m^2\alpha^2 T_0 \Delta T_g}{2R_g} + \frac{P_{out}}{2} \right) \quad (7)$$

where  $T_0$  and  $T_1$  are the temperatures at the cold and hot side of the entire device, respectively.

Inserting Eqs. (6) and (7) in Eq. (3) leads to a cubic equation in  $\Delta T_g$  with three real solutions for physically valid parameters. As two of these solutions imply negative temperature values for  $T_c$ , only the third solution is of physical significance. When this solution for  $\Delta T_g$  is inserted in Eq. (2), an expression of the maximum electrical power output of the generator is obtained which depends on the external temperatures  $T_0$  and  $T_1$ , the material properties and geometry only. This result reveals that a micro-scale TEG ( $\mu$ -TEG) operates in another regime than conventional large-scale TEGs (see Fig. 3). For the sake of brevity, the explicit expression of the solution cannot be given here because of its complicated shape.

## 2.2. Simplified model

If the heat contributions by the Peltier effect and Joule heating are neglected in Eqs. (4) and (5), Eq. (3) can easily be solved for  $\Delta T_g$ :

$$\Delta T_g = \frac{K_g}{K_g + K_c + K_h} \Delta T \quad (8)$$

Using Eq. (2), an expression of the maximum electrical power output is obtained:

$$P_{out} = \frac{m^2\alpha^2}{4R_g} \left( \frac{K_g}{K_g + K_c + K_h} \Delta T \right)^2 \quad (9)$$

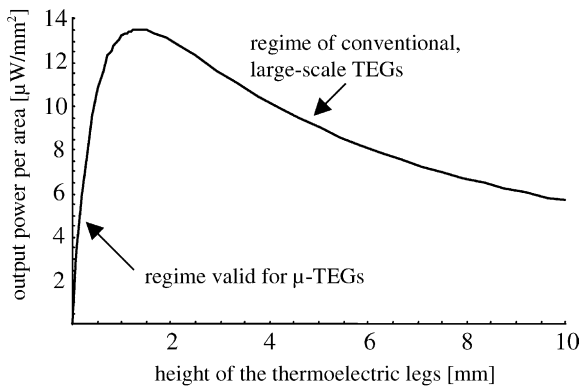


Fig. 3. Calculated output power of a typical TEG as a function of the height  $t$  of the thermoelectric legs.  $\mu$ -TEGs are operated in the regime shown on the left.

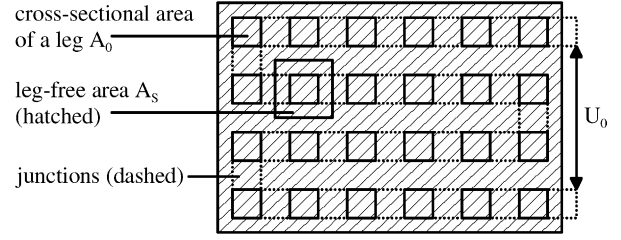


Fig. 4. Schematic top-view of a TEG arranged in meanders. See text for notation.

As the generator consists of meanders of thermoelectric couples (see Fig. 4) and the heat flux is in vertical direction, its elements are thermally connected in parallel. If the biggest part of the heat flows through the thermoelectric legs, i.e. for  $\lambda \gg \lambda_s$  where  $\lambda = (\lambda_n + \lambda_p)/2$  is the mean thermal conductivity of a thermocouple and  $\lambda_s$  is the thermal conductivity of the gaps between the couples, the thermal resistance  $K_g$  of the generator reduces to

$$K_g = \frac{t}{2m\lambda A_0} \quad (10)$$

where  $t$  denotes the thickness of the generator layer and  $A_0$  is the cross-sectional area of a thermoelectric leg.

For thin generator layers holds the estimate  $K_g \ll K_c + K_h$ . According to Eq. (2), Eq. (10) and with  $2\rho mt/A_0$  substituted for the electrical resistance  $R_g$ , the output power  $P_{out}$  becomes

$$P_{out} = \frac{1}{32} \frac{\alpha^2}{\lambda^2 \rho} \frac{t}{mA_0} \left( \frac{\Delta T}{K_c + K_h} \right)^2 \quad (11)$$

where  $\rho = (\rho_n + \rho_p)/2$  is the mean electrical resistivity of a thermocouple.

As the enclosing thermal resistors are dependent of the total area of the generator  $A_g = 2m(A_0 + A_s)$ , they can also be understood as cubic thermal resistors  $K_c = t_c/(\lambda_c A_g)$  and  $K_h = t_h/(\lambda_h A_g)$ :

$$P_{out} = \frac{1}{16} \frac{\alpha^2}{\lambda^2 \rho} t \frac{A_0 + A_s}{A_0} \frac{\lambda_c^2 \lambda_h^2}{(t_c \lambda_h + t_h \lambda_c)^2} (\Delta T)^2 A_g \quad (12)$$

Here,  $\lambda_c$  and  $\lambda_h$  are the thermal conductivities and  $t_c$  and  $t_h$  the thicknesses of the thermal resistors on the cold and hot side, respectively.  $A_s$  denotes the free area between neighboring legs in a unit cell.

This result shows that the maximum output power per area of a  $\mu$ -TEG, i.e. a generator consisting of thermoelectric legs that are some few  $\mu\text{m}$  high, is limited by the Seebeck coefficient  $\alpha$ , the electrical resistivity  $\rho$  and the thermal conductivity  $\lambda$ .  $P_{out}$  increases with the height  $t$  of the thermoelectric couples and it decreases with the cross-sectional area  $A_0$  of the legs. The above relation for maximum power output also suggests to define a modified figure of merit,  $Z^*$ , characterizing the performance of a  $\mu$ -TEG as

$$Z^* = \frac{Z}{\lambda} = \frac{\alpha^2}{\lambda^2 \rho} \quad (13)$$

Since the square of the thermal conductivity  $\lambda$  enters this expression, the importance of a high internal thermal resistivity of a  $\mu$ -TEG is evident. Hence, this modified figure of merit  $Z^*$  is an appropriate criterion to find suitable materials for micro-scale thermoelectric devices.

For the derivation of the modified figure of merit  $Z^*$  as introduced above the contact resistances  $R_c$  of the metal junctions have been neglected. To describe the system for non-vanishing  $R_c$  the electrical resistance of the generator would be

$$R_g = mR_{\text{cell}} = m(2R_{\text{leg}} + 4R_c) \quad (14)$$

Note that each thermocouple implies four metal contacts. It will be discussed below that the contact resistances can amount up to more than half of the total electrical resistance.

### 3. Material properties

The Seebeck coefficient  $\alpha$ , the electrical resistivity  $\rho$  and the thermal conductivity have been measured for both pure poly-Si and poly-Si<sub>70%</sub>Ge<sub>30%</sub> (see Table 1). The Seebeck

coefficients have been extracted using special planar test structures [5]. The values of the electrical resistivity have been determined from van-der-Pauw Greek crosses [6]. A novel test vehicle was designed to measure the thermal conductivities of the poly-Si layers.

For producing this thermal test structure, the poly-Si layer is patterned into two sets of beams and a heater connecting them (see Fig. 5). The 1.6  $\mu\text{m}$  thick sacrificial oxide layer underneath the poly-Si is removed using HF etchant. Hence, a cavity is created below the actual device.

Applying an electrical current to the poly-Si heater, most of the generated heat  $P_{\text{el}} = UI$  is forced to flow into the beams perpendicular to it. As an analytical calculation reveals, the electrical heating power has to be reduced by the heat lost in the connections of the heater, yielding the correct amount of heat  $P_c$  flowing into the beams:

$$P_c = \gamma P_{\text{el}}$$

$$\text{with } \gamma = \frac{2nw(n^2w^2 + 6nwq + 6q^2)}{2n^3w^3 + 12n^2w^2q + 6glq + 3nwg\ell + 12nwq^2} \quad (15)$$

Table 1  
Measured material properties for 400 nm thick poly-Si and poly-SiGe layers

Material	Doping concentration $c$ ( $\text{cm}^{-3}$ ) ( $\times 10^{20}$ )	Seebeck coefficient $\alpha$ ( $\mu\text{V/K}$ )	Electrical resistivity $\rho$ ( $\text{m}\Omega \text{ cm}$ )	Thermal conductivity $\lambda$ ( $\text{W/m K}$ )	Figure of merit $Z^*$ ( $\mu\text{m/W}$ ) <sup>a</sup>
n-Poly-Si	2.5	$-57 \pm 9$	$0.813 \pm 0.001$	$31.5 \pm 3.7$	0.4
p-Poly-Si	2.5	$103 \pm 17$	$2.214 \pm 0.004$	$31.2 \pm 3.7$	0.5
n/p-Poly-Si couples	2.5	$160 \pm 19$	$1.514 \pm 0.004$	$31.4 \pm 5.2$	1.7
n-Poly-SiGe	2.5	$-77 \pm 7$	$2.37 \pm 0.04$	$9.4 \pm 2.0$	2.8
p-Poly-SiGe	2.5	$59 \pm 9$	$1.87 \pm 0.01$	$11.1 \pm 2.0$	1.5
n/p-Poly-SiGe couples	2.5	$136 \pm 11$	$2.12 \pm 0.04$	$10.3 \pm 2.8$	8.2

<sup>a</sup>  $Z^*$  is calculated according to Eq. (13).

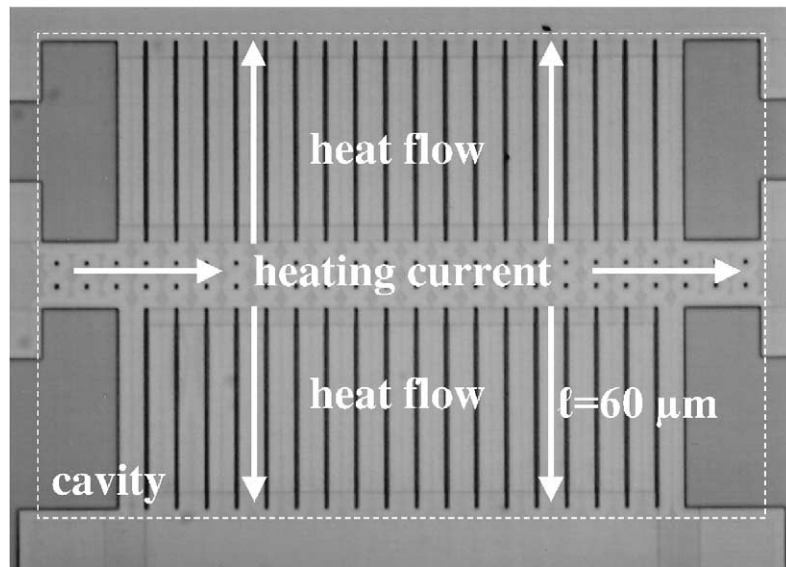


Fig. 5. Micrograph of a double-beam test structure to measure the thermal conductivity of poly-Si layers. The boundary of the cavity underneath the device is indicated by dashed lines.

where  $\ell$  is the length of a beam,  $n$  the number of beams,  $w$  is the width of a beam and  $q$  and  $g$  are the length and the width of a connection of the poly-Si heater, respectively.

In that way, measuring under vacuum conditions, the thermal conductance of the beams and, thus, the thermal conductivity of the poly-Si itself can be deduced according to the relation [7]:

$$\lambda = \frac{P_c R(T_0) \beta \ell}{nw \Delta R t} \quad (16)$$

where  $R(T_0)$  is the initial electrical resistance,  $\beta$  the temperature coefficient of resistance,  $\Delta R = R(T_0) \beta \Delta T$  is the resistance change and  $t$  is the thickness of the layer.

The advantage of this surface micromachined thermal structure compared to previously presented ones [8] is not only the fact that it does not require any bulk micromachining but mainly the novelty that the actual poly-Si layer to be investigated is no sandwich with other materials, namely oxide.

Using this structure, the thermal conductivities of poly-Si and poly-Si<sub>70%</sub>Ge<sub>30%</sub> have been measured (see Table 1). As expected [8–10], the benefit of poly-SiGe is based on its lower thermal conductivity compared to pure poly-Si. Hence, poly-Si<sub>70%</sub>Ge<sub>30%</sub> turns out to be more promising for use in our TEGs because of its higher figure of merit. However, in agreement with earlier work [11], the electrical resistivity of phosphorus-doped poly-SiGe was found to be higher than that of identically n-doped pure poly-Si. This finding limits the gain in performance of poly-SiGe as thermoelectric material because it leads to a higher total electrical resistance of the generator.

#### 4. Device realization

The generators were fabricated in a BiCMOS production facility, each one consisting of 59,400 thermocouples integrated on an area of about 6 mm<sup>2</sup>. A schematic view onto the cells of the generator is displayed in Fig. 6. The thermal isolation between the cold and the hot side of the thermoelectric legs is achieved by means of a 1.6  $\mu$ m thick thermal barrier made of LOCOS oxide. A 400 nm thick poly-Si layer is partially phosphorus-implanted with an energy of 130 keV to generate the n-legs and partially boron-implanted using 40 keV in other regions to form the p-legs, both employing a dopant dose of 10<sup>16</sup> cm<sup>-2</sup>. Afterwards, the poly-Si layer is patterned to release the thermoelectric legs.

Both, samples with pure poly-Si as well as others containing poly-Si<sub>70%</sub>Ge<sub>30%</sub> have been produced. The poly-SiGe layers were grown in a conventional chemical vapor deposition (CVD) reactor, commonly used for poly-Si deposition. For the deposition a mixture of disilane (Si<sub>2</sub>H<sub>6</sub>) and germane (1% GeH<sub>4</sub> in H<sub>2</sub>) was used. The carrier gas was hydrogen. The poly-SiGe layers were grown at a temperature of 670 °C and a pressure of 19 Torr. With these parameters a high deposition rate of 100 nm/min was achieved. To avoid big grains that may result from an insufficient nucleation of germanium on oxide, a thin poly-Si wetting layer of about 5 nm was deposited prior to the deposition of poly-SiGe. Aluminum bridges are used to avoid n/p-junctions which otherwise would exist between adjacent thermoelectric legs. A second metal bridge is added to every other junction to improve the thermal coupling to the surface of the device. Moreover, in order to optimize the heat flux direction within

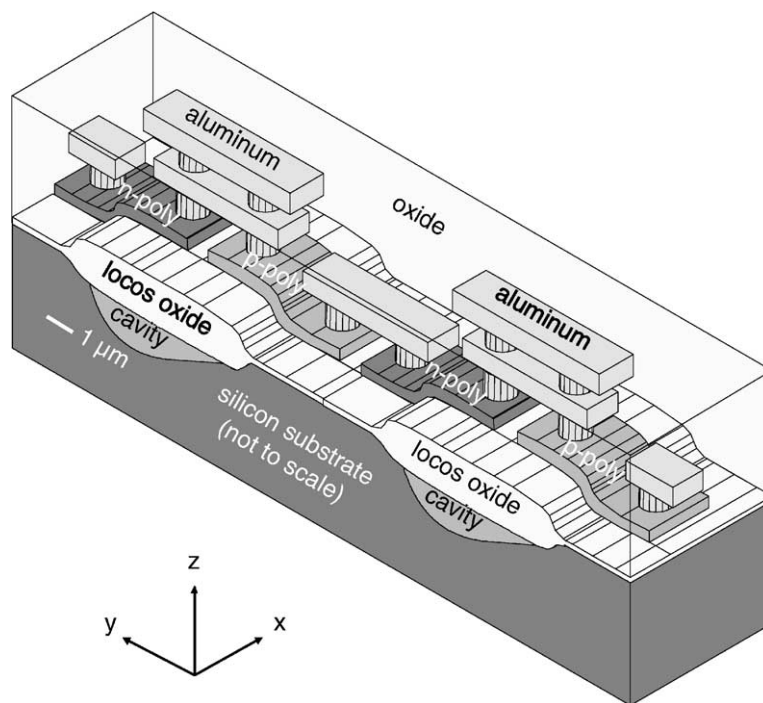


Fig. 6. Schematic view of two thermoelectric couples of the BiCMOS realization. Additionally, the cavities which can be etched into the Si-substrate are shown.

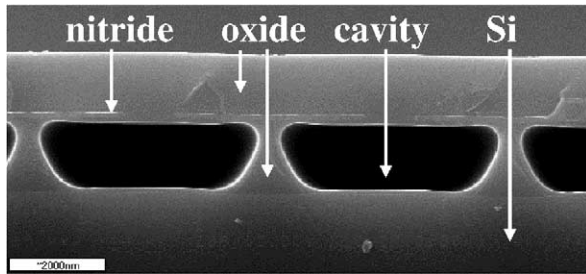


Fig. 7. Cavities etched into the oxide barrier using buffered HF. The holes in the nitride mask were re-closed with oxide after etching. View along the y-direction of Fig. 4.

the generator, two different micromachining steps have been explored. In a first attempt, the oxide barriers below the poly-Si stripes have been removed through the common technique of buffered HF wet etching (see Fig. 7). To define the regions to be etched, the sacrificial oxide layer has to be covered with a nitride mask perforated with holes. In a second approach, cavities have been etched into the silicon substrate using isotropic  $\text{CF}_4$  dry etching (see Figs. 6 and 8). The poly-Si legs are protected by an oxide mask during etching.

## 5. Results

The devices have been tested on wafer-level, placed on a heatable thermochuck and a cooler mounted on top. In agreement with the results of the thermal simulations previously performed using the FEM tool ANSYS [5], the micromachining steps improved the output voltage of the generator significantly. The use of poly-SiGe combined with substrate etching doubled the open-circuit voltage compared to the basic type. An output efficiency of between 100 and 200 mV/K could be obtained. Measured output voltages per area for each type of TEG are shown in Fig. 9. The electrical resistances of the thermoelectric legs, the electrical contacts and the entire generator cells are summarized in Table 2. For the poly-Si generator type, nearly half of the total resistance of about 10 M $\Omega$  results from the contacts. In the case of poly-SiGe, the resistance of the contacts was found to be even more dominating. As the electrical resistivity of n-doped poly-SiGe is undesirably high, too, measures have to be taken to reduce those resistances. Experiments focusing on these matters are in progress.

Obviously, the output power is mainly limited by the electrical resistance of the generators. Therefore, the poly-SiGe generators cannot outdo the pure poly-Si types. A

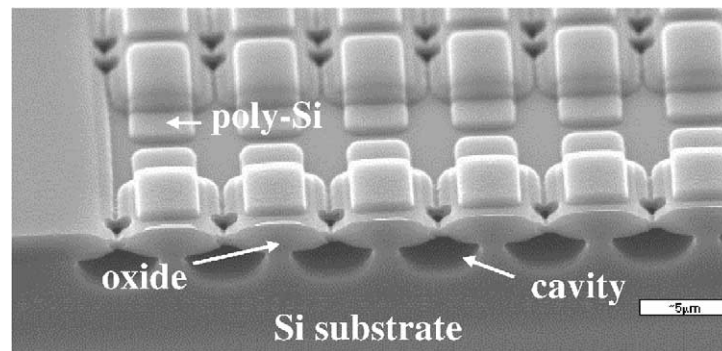


Fig. 8. SEM micrograph showing cavities etched into the Si-substrate using  $\text{CF}_4$  dry etchant. View before metallization along the y-direction as displayed in Fig. 4.

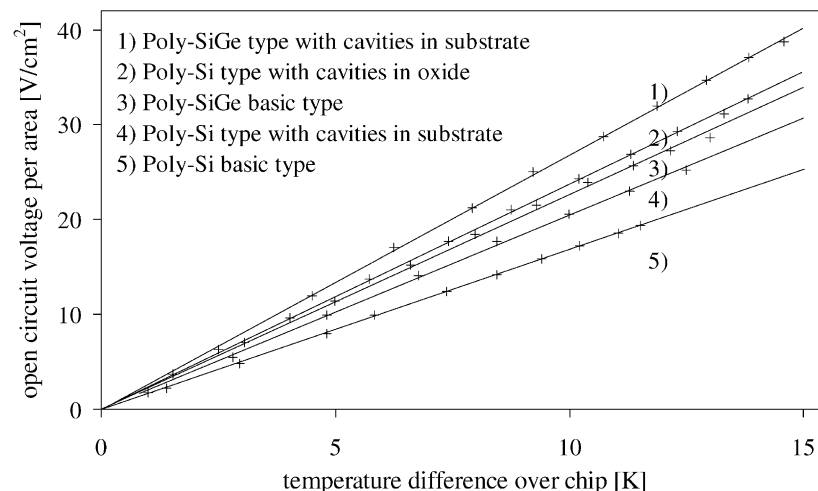


Fig. 9. Measured open-circuit voltages per area of the different generator types vs. the temperature drop between bottom and top of the entire chip.

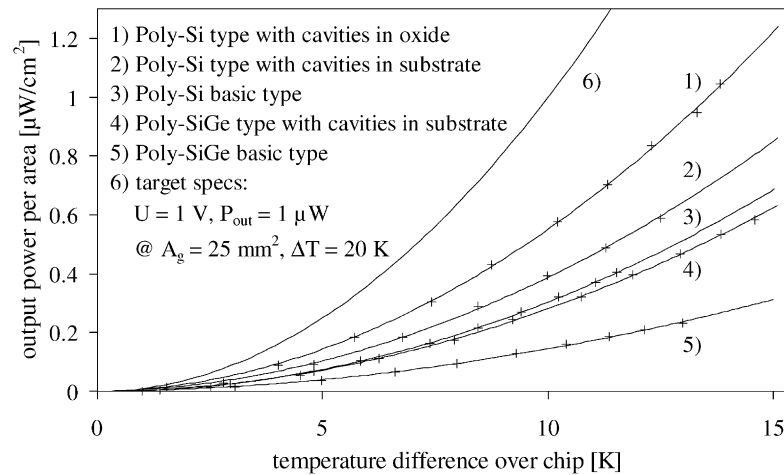


Fig. 10. Measured output power per area of the different generator types vs. the temperature drop between bottom and top of the entire chip.

Table 2

Electrical resistances  $R_{\text{leg}}$  of a leg,  $R_c$  of a contact and  $R_{\text{cell}}$  of an entire cell of the poly-Si and poly-SiGe type TEG, respectively

Material	Electrical resistance		
	$R_{\text{leg}}$ ( $\Omega$ )	$R_c$ ( $\Omega$ )	$R_{\text{cell}}$ ( $\Omega$ )
Poly-Si	$54 \pm 1$	$23 \pm 1$	$202 \pm 5$
Poly-SiGe	$76 \pm 1$	$119 \pm 4$	$629 \pm 19$

graph of the output power per area versus the temperature difference for the presented generator types is displayed in Fig. 10. For comparison, the target specifications are given. The aim is to build a generator supplying 1 V under load and 1  $\mu\text{W}$  output power at a temperature difference of 20 K placed on an area of not more than 25  $\text{mm}^2$ .

## 6. Conclusion

The difference between conventional large-scale TEGs and  $\mu\text{-TEGs}$  has been elaborated. A modified figure of merit  $Z^*$  for  $\mu\text{-TEGs}$  has been proposed which stresses the importance of a high internal thermal resistance of the generator.  $Z^*$  can be used as a valuable criterion to find suitable materials for these specific thermoelectric devices. The Seebeck coefficient  $\alpha$ , the electrical resistivity  $\rho$  and the thermal conductivity  $\lambda$  have been measured for both pure poly-Si and poly-Si<sub>70%</sub>Ge<sub>30%</sub>. A novel test structure for determining the thermal conductivity of poly-Si layers has been presented. In order to optimize the heat flow within the device, special surface micromachining techniques have been explored. Generators of 6  $\text{mm}^2$  size made of poly-Si as well as poly-SiGe have been fabricated in our facility and were tested successfully. The open-circuit voltage was in the range between 100 and 200 mV/K. Further efforts will still have to be made in order to reduce the electrical resistance of the generators because it limits the achievable output power.

## References

- [1] M. Kishi, H. Nemoto, M. Yamamoto, S. Sudou, M. Mandai, S. Yamamoto, Micro-thermoelectric modules and their application to wrist-watches as an energy source, in: Proceedings of the IEEE 18th International Conference on Thermoelectrics, 1999, pp. 301–307.
- [2] R.R. Heikes, R.W. Ure, Thermoelectricity: Science and Engineering, Interscience, New York, 1961.
- [3] A.W. Culp, Principles of Energy Conversion, McGraw-Hill, New York, 1991.
- [4] G. Min, R.W. Rowe, Peltier devices as generators, in: D.M. Rowe (Ed.), CRC Handbook of Thermoelectrics, CRC Press, Boca Raton, 1995.
- [5] M. Strasser, R. Aigner, G. Wachutka, Analysis of a CMOS low power thermoelectric generator, in: Proceedings of Eurosensors XIV, 2000, pp. 17–20.
- [6] M.I. Newsam, A.J. Walton, M. Fallon, Numerical analysis of the effect of geometry on the performance of the Greek cross structure, in: Proceedings of the IEEE International Conference on Microelectronic Test Structures'96, Vol. 9, 1996, pp. 247–252.
- [7] F. Völklein, Characterization of the thermal properties of bulk and thin-film materials by using diagnostic microstructures, in: Proceedings of the Micrometrology Symposium, Delft, The Netherlands, 31 August–1 September 2000, pp. 91–107.
- [8] M. von Arx, O. Paul, H. Baltes, Process-dependent thin-film thermal conductivities for thermal CMOS MEMS, J. Microelectromech. Syst. 9 (1) (2000) 136–145.
- [9] C.B. Vining, Silicon/germanium, in D.M. Rowe (Ed.), CRC Handbook of Thermoelectrics, CRC Press, Boca Raton, 1995.
- [10] P. Van Gerwen, K. Baert, R. Mertens, Thin-film poly-Si<sub>70%</sub>Ge<sub>30%</sub> for thermopiles, in: Proceedings of the Microsystem Technologies'98, Potsdam, Germany, 1–3 December 1998, pp. 655–658.
- [11] D.S. Bang, M. Cao, A. Wang, K.C. Saraswat, Resistivity of boron and phosphorus-doped polycrystalline Si<sub>1-x</sub>Ge<sub>x</sub> films, Appl. Phys. Lett. 6 (2) (1995) 195–197.

## Biographies

M. Strasser was born in Düsseldorf, Germany, in 1972 where he studied physics at Heinrich Heine University. In 1998, he finished his diploma degree at Siemens Semiconductors in Munich doing research in electromigration of CMOS metallizations. Since 1998, he is working towards his DSc degree at Munich University of Technology and is with the MEMS group of Infineon Technologies AG. His current main research

interests are the thermoelectric properties of BiCMOS materials and the development of integrated thermoelectric devices.

*R. Aigner* received his PhD degree from Munich University of Technology, in 1996 for research on micromachined chemical sensors. He was a visiting scientist at Berkeley Sensors and Actuators Center BSAC, in 1996 where he worked on system design for inertial sensors. After that he joined the research group for MEMS at Siemens Corporate Technology, in 1997. Since 1999, he is responsible for MEMS research at Infineon Technologies. His activities have a focus on advanced automotive sensors and MEMS for communication technologies. As a representative for his company he is member of several European institutions and committees for microsystem technology and was recently nominated as MEMS expert for European Commission's research projects.

*M. Franosch* received his diploma in physics at Munich University of Technology (in collaboration with GSI, Darmstadt) for research in nuclear physics, in 1985. Until 1985, he continued this work as scientific assistant at Munich University of Technology. In 1986, he joined the new e-beam group at the Siemens Corporate Research and Development Department. From 1990 to 1992 he was doing research on phase shift masks. Since 1992, he is working in process development of silicon-, silicon/germanium- and germanium-CVD processes for different bipolar and CMOS applications and micromechanical sensors. Since 1999, he is a member of the MEMS group at Infineon Technologies.

*G. Wachutka* received the DSc degree from the Ludwig-Maximilians-Universität, Munich, Germany, in 1985. From 1985 to 1988, he was with Siemens Corporate Research and Development, Munich, where he headed a modeling group active in the development of modern high-power semiconductor devices. In 1989, he joined the Fritz-Haber-Institute of the Max-Planck-Society, Berlin, Germany, where he worked in the field of theoretical solid-state physics. From 1990 to 1994, he was head of the micro-transducers modeling and characterization group of the Physical Electronics Laboratory at the Swiss Federal Institute of Technology (ETH), Zurich. There, he also directed the micro-transducers modeling module of the Swiss Federal Priority Program M2S2 (Micromechanics on Silicon in Switzerland). Since spring 1994, he has been heading the Institute for Physics of Electrotechnology at the Munich University of Technology, where his research activities are focused on the design, modeling, characterization, and diagnosis of the fabrication and operation of semiconductor microdevices and microsystems. He has authored or co-authored more than 180 publications in scientific or technical journals. He is consultant of research institutes in industry and university, and he serves as reviewer for various scientific journals and other institutions. Among his many educational activities, he has set up and taught courses funded by European Community training programmes such as UETP, EUROFORM, and EUROPRACTICE. Prof. Wachutka is member of the IEEE, the American Electrochemical Society, the American Materials Research Society, the ESD Association, the German Physical Society, and the AMA Society for Sensorics.